1-1-2011

Nano-Patterned High-Responsivity GaAs Metal-Semiconductor-Metal Photodetector

Ayman Karar
Edith Cowan University, ayman_karar@hotmail.com

Chee Leong Tan

Kamal Alameh
Edith Cowan University, k.alameh@ecu.edu.au

Yong Tak Lee

10.1109/HONET.2011.6149782
This is an Author's Accepted Manuscript of: Karar, A. , Tan, C., Alameh, K. , & Lee, Y. (2011). Nano-patterned high-responsivity GaAs metal-semiconductor-metal photodetector. Paper presented at High-Capacity Optical Networks and Enabling Technologies (HONET) 2011, Riyadh, Saudi Arabia. Available here

Nano-patterned High-responsivity GaAs Metal-Semiconductor-Metal Photodetector

Ayman Karar[1*], Chee Leong Tan[2], Kamal Alameh[1,4]* and Yong Tak Lee[2,3,4]

[1]Electron Science Research Institute, Edith Cowan University, Joondalup, WA, Australia

[2]School of Photonics Science, Gwangju Institute of Science and Technology (GIST), Gwangju 500-712, Republic of Korea

[3]Department of Information and Communications, GIST Republic of Korea

[4]Department of Nanobio Materials and Electronics, World Class University, Gwangju Institute of Science and Technology, Gwangju 500-712, Republic of Korea

Phone: +61 8 6304 5836, Fax: +61 8 6304 5302, *email: k.alameh@ecu.edu.au, a.karar@ecu.edu.au

***Abstract*—In this paper, we use the finite difference time-domain (FDTD) method to optimize the light absorption of an ultrafast nano-grating plasmonic GaAs metal-semiconductor-metal photodetector (MSM-PD) employing double metal nano-gratings. The geometry of the MSM-PD is theoretically investigated, leading to improved light absorption near the design wavelength of GaAs due to plasmon-assisted electric and magnetic field concentration through a subwavelength aperture. Simulation results show up to 8- and 21-times light absorption enhancement for the single and double nano-grating structure, respectively, in comparison to conventional MSM-PDs. Experimentally, more than 4 times enhancement in photocurrent is demonstrated for a single top nano-grating MSM-PD in comparison with conventional MSM-PDs.**

***Index Terms*— Subwavelength aperture, surface plasmon polaritons , FDTD simulation, MSM-PD.**

I. INTRODUCTION

The monolithic design, integration with standard VLSI circuitry, high speed performance, and applicability to 2-D array layouts make the metal semiconductor metal photodetector (MSM-PD) a good candidate for several applications such as high-speed optical interconnect, high-speed sampling, and optical fiber communication system components[1-2]. Due to their lateral geometry, MSM-PDs have much smaller capacitance per unit area in comparison to standard p-i-n photodiode with same active area. The surface reflectivity and the shadowing due to the metal fingers prevent an ideal MSM-PD from achieving external quantum efficiency greater than 50% for equal electrode width and spacing. The smaller finger width, the less detector capacitance and the shorter external response time [3]. By decreasing the spacing between the electrode fingers down to the optical diffraction limit, the response times could be in the range of a few tens of picoseconds [4]. However, this downsizing of the electrode spacing decreases the active area, thus resulting in photodetector sensitivity degradation.

After the Extraordinary Optical Transmission (EOT) phenomenon was first reported by Ebbesen et al. [5], many efforts have been devoted to exploring the EOT through metallic gratings with various sub-wavelength structures, such as periodic slit arrays, hole arrays, and corrugated metal films for different wavelength regions [6]. Recently, It has also been established that the transmission of light through a hole (or slit) in a metal film can be enhanced by microstructuring the top or bottom surfaces of the film with gratings. These gratings couple the incident light to surface plasmon polaritons (SPPs) that are guided into the holes [7-9].

Metallic corrugation patterned as a periodic grating has been designing to improve HgCdTe [10] and angled incidence quantum-well infrared photodetectors (QWIPs) [11]. A new technique has been reported by Collin et al. [12] for efficient light absorption in MSM-PDs. They confirmed that the confinement of light in subwavelength metal–semiconductor gratings can be achieved by Fabry–Pérot resonances involving vertical transverse magnetic and electric guided waves, thereby increasing the quantum efficiency. Recently, we reported a semi-analytical model of light absorption around 830 nm for MSM-PDs with top plasmonic nano-gratings using the finite difference time domain (FDTD) numerical method [13]. In that report, we showed that the transmission enhancement strongly depends on several parameters of the device structure, such as, the shape, height and nano-grating period, as well as, the sub-wavelength aperture width.

In this paper, using FDTD method, we continue the work reported in previous paper [13] to investigate the transmission enhancement of a plasmonics-based double grating subwavelength aperture MSM-PD structure and compare its performance to a single subwavelength aperture and top nano-grating subwavelength aperture MSM-PDs structure. In depth analyses of the electromagnetic field distributions across the MSM-PD structure are presented, and the optimized metallic grating dimensions for maximizing the optical transmission enhancement.

Our simulation results show that the double nano-grating plasmonic MSM-PD structure can attain 21-times better absorption than conventional MSM-PDs and more than 2 times with the top nano-grating plasmonics-based MSM-PD, and this is mainly due to the extraordinary optical signal propagation through the bottom metal nano-gratings.

II. Double nano-grating MSM-PDs

To maximize the light concentration effects, we combine two distinct mechanisms that relate to the presence of the subwavelength aperture and the nano-gratings. The metallic subwavelength aperture supports a propagating TE mode with the EOT. Consequently, with an appropriate choice of its width, the subwavelength aperture forms a Fabry–Pérot resonator; therefore, the light transmission through the subwavelength aperture is resonantly enhanced. On the other hand, the nano-gratings enhance the light transmission through the subwavelength aperture region by converting the incident EM waves into SPs propagating on the metal surface, which can be funneled into the subwavelength aperture [14].

For the design of an MSM-PD structure, we used the FDTD method to explore the application of SPs to improve the light transmission through a subwavelength aperture. A conventional MSM-PD structure is shown in Fig. 1(a). It consists of a two metallic (Au) contacts separated by a subwavelength aperture of width X_w. Fig. 1(b) shows a 2D plasmonic MSM-PD structure consisting of a subwavelength aperture sandwiched between top linear metal nano-gratings h_{tg} of a period Λ. Fig. 1(b) also shows the bottom metal nano-grating parameters with bottom nano-grating height h_{bg} with period Λ_b, while Fig. 1(c) shows a 3D plasmonic MSM-PD consist of the linear metal nano-grating on top and bottom. The metal layers are grown on top of a semiconductor (GaAs) substrate.

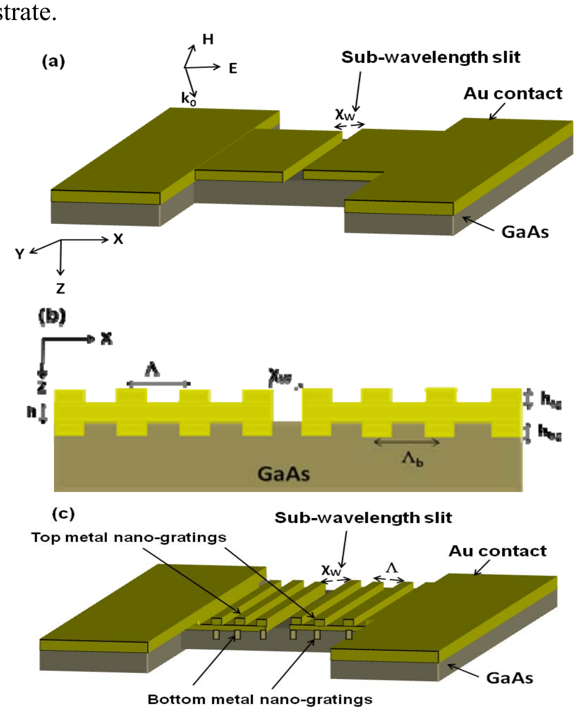

Fig. 1: (a) Simple MSM-PD structures: (a) without, (b) 2D and (c) 3D with double linear plasmonic nano-grating.

To design the MSM-PDs (with and without metal nano-gratings), we used a 2D FDTD models software that was developed by Optiwave Inc [15]. The structure had a mesh step size of 2 nm in both x- and z- directions while the time step satisfy the condition of $\delta t < 0.1\delta x/c$. This high-resolution sampling yielded solutions that converged at reasonable computation times. The excitation field was modeled as a Gaussian-modulated continuous wave in the z-direction. The anisotropic perfectly matched layer (APML) boundary conditions were applied in both the x- and z- directions to accurately simulate the light reflected from the bottom and both sides, as well as light transmitted from the top boundaries of the MSM-PD structure. The gold (Au) dielectric permittivity was defined by the Lorentz-Drude model [16] and the GaAs dielectric permittivity data was taken from [17]. It is important to mention here that, for all simulation the subwavelength aperture, top nano-grating height (h_{tg}), and period (Λ), duty cycle, number of period were kept constant at 100 nm, 120 nm, 815 nm, 50% and 7 respectively, for more details see Ref (13).

By defining a term called light transmission enhancement factor (Γ), which is the calculated light power transmission of the device with the double nano-grating divided by that without the nano-grating, we can give a concise expression for the increase in transmitted power into the active area for the same device with and without the nano-gratings.

Firstly, the bottom height of the nano-grating, h_{bg}, the duty cycle, and the number of period were kept at 100 nm, 50% and 7 respectively, while the bottom nano-grating periodicity, Λ_b was varied from 400 nm to 1000 nm. Simulation results show that the bottom nano-grating period almost has no effect on the transmission enhancement factor spectrum. This result is similar to the one reported by F.J. Garcia-Vidal et.al for double plasmonic nano-grating on air [18].

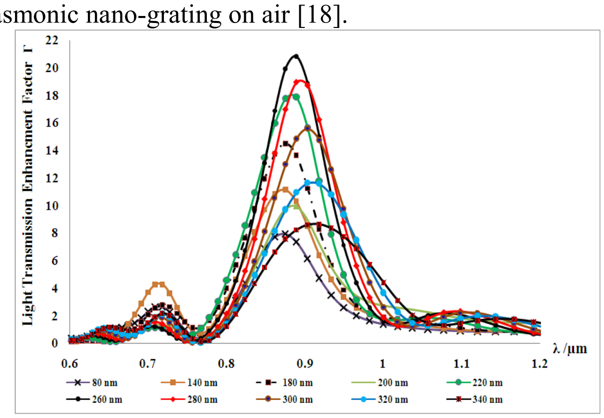

Fig. 2: Light transmission enhancement factor for x_w = 100 nm for different nano-grating heights h_{Bg}.

Another design was simulated, where the same previous parameters were used with a nano-grating period of 815 nm, while the bottom nano-grating height h_{bg} was varied from 40 nm to 340 nm. Fig. 2 shows the transmission spectrum for different bottom nano-grating heights. It is obvious from Fig. 2 that the nano-grating height has a significant impact on the amount of power transmitted into the semiconductor area. The maximum transmission enhancement of 21-times is obtained at h_{bg} = 260 nm. Another interesting observation can be recognized from these spectra that the central position of the optimum wavelength is red-shifted after the maximum enhancement at 260 nm nano-grating height. The maximum transmission is at 887 nm, which is not the design wavelength of the nano-gratings. However, this wavelength still falls within the absorption range of GaAs.

In order to complete study of the double nano-grating MSM-PD structure, the bottom nano-grating duty cycle was varied from 10% to 90% in steps of 10%, while the bottom nano-grating heights h_{bg} was kept at 260 nm. Fig. 3 shows the Γ spectra for different duty cycle. It is noticed that the duty cycle has a negligible affect on the transmission enhancement factor.

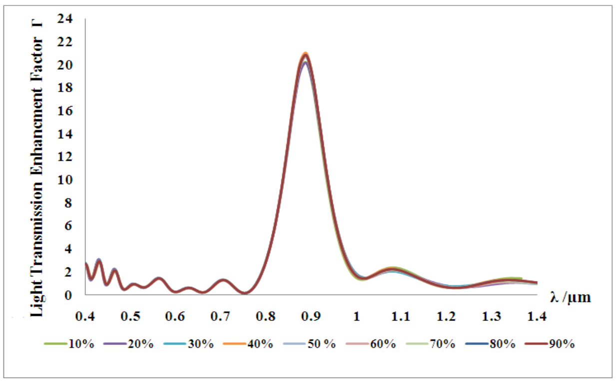

Fig. 3: Light transmission enhancement factor for $\mathbf{x_w}$ = 100 nm with varying bottom nano-grating duty cycle.

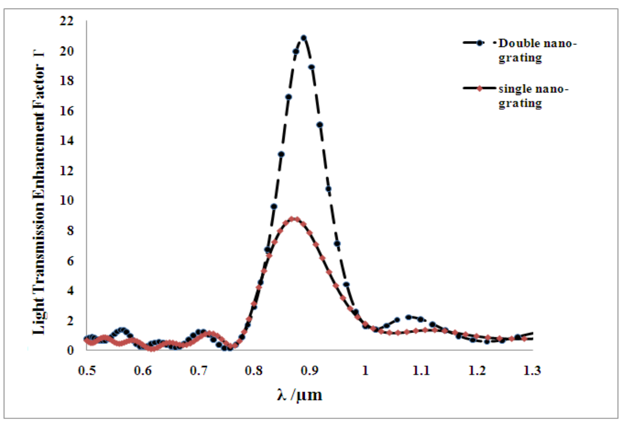

Fig. 4: Light transmission enhancement factor spectrum for the double and single nano-grating plasmonic MSM-PD device.

The optimized device was subsequently simulated using the parameters determined in the previous sections, which are: i) subwavelength aperture width of 100 nm, ii) bottom nano-grating height of 260 nm, iii) nano-grating duty cycle of 50%, and iv) number of the nano-grating periods of 7. The light enhancement transmission spectra for the optimized double nano-grating plasmonic MSM-PD device and the single top nano-grating MSM-PD are shown in Fig. 4.

From Fig. 4, it is observed that the light transmission enhancement factor is 21-times, however, the peak wavelength is shifted to 887 nm, whereas the enhancement factor is around 8-times for the top nano-grating plasmonics-based MSM-PD and the wavelength is 876 nm at the maximum enhancement.

The computed electric and magnetic field distribution components ($|E_x|$, $|H_y|$, and $|E_z|$) for the MSM-PDs with and without the double nano-grating are shown Fig. 5.

As shown in Fig, very little E_x is needed on the top surface to sustain the surface current J_x, which supports the magnetic field H_y immediately above the surface. The reflected E_x and H_y interfere with the corresponding incident fields to produce standing waves above the top surface. J_x stops abruptly at the edge of the slit, giving rise to accumulated charges at the sharp corners, where these oscillating charges on opposite edges of the slit behave as an electric dipole.

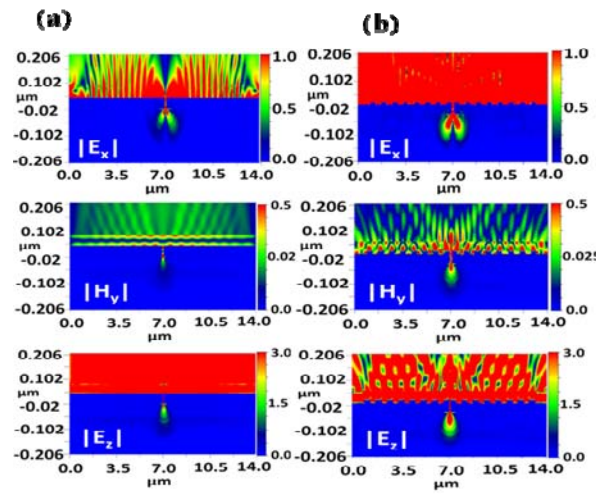

Fig. 5: Field distributions ($|E_x|$, $|H_y|$ and $|E_z|$) of the optimized device without nano-grating (a) and with the double nano-grating (b).

These field distributions clearly show the SPP coupling effects and the light transmission enhancement through the subwavelength aperture with the incorporation of the nano-grating. Fig. 5 shows that a small fraction of the EM fields are transmitted into the active area of the device without the nano-grating in compression with the one with double nano-grating. Moreover, the H_y field distribution for the device with the double nano-grating clearly shows the presence of a TM polarized wave propagating along the surface, as predicted by the SPP coupling theory [19].

III. Experimental results

Fig. 6(a) shows an SEM image of fabricated top metal nano-grating plasmonics-based MSM-PD structure fabricated with focused ion beam lithography FIB on top of GaAs substrate. The inset shows a high magnification image of the sub-wavelength slit with linear Au nano-gratings at both sides with period of 866 nm and slit width of 231 nm. Fig. 1(b) shows the measured I-V characteristics for two developed plasmonic MSM-PDs, one with top nano-gratings etched onto the metal fingers, and the other (traditional MSM-PD) without nano-grating (denoted as WG and WOG, respectively), for an input laser power of 5 mW at 830 nm. Referring to Fig. 1(b), it is clear that the plasmonics-based MSM-PD structure produces a 4 times higher photocurrent at optimum bias voltage of 0.5 V in comparison to the traditional MSM-PD without nano-gratings. Note that in Fig. 4, the theoretical enhancement in transmission is 8 times (for top nano-gratings). The discrepancy (factor of 2) between the theoretical and experimental results is attributed to (i) the grating phase shift near the slit and (ii) the trapezoidal shape of the nano-grating grooves both reducing the transmission enhancement as reported by Das et al. [20, 21].

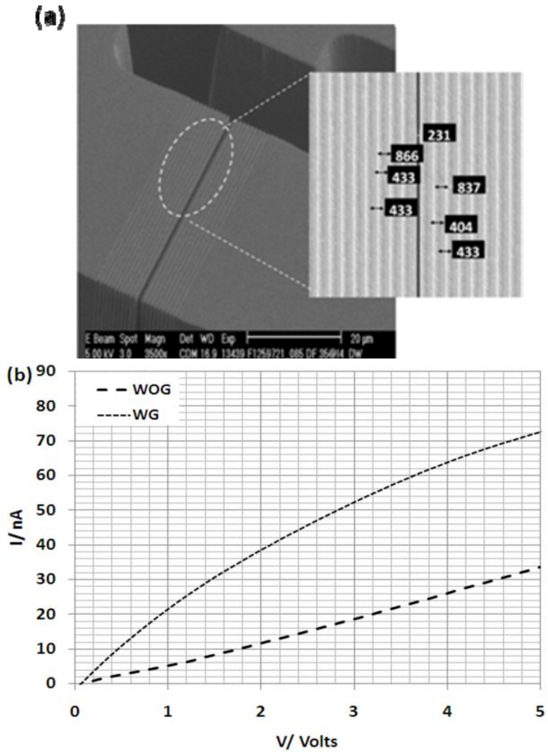

Fig 6: (a) An SEM image of the fabricated plasmonics-based MSM-PD structure. (b) Measured I-V characteristics comparing GaAs MSM-PDs with top nano-gratings (WG) and without nano-gratings (WOG) for an input laser power of 5 mW at 830 nm.

IV. Conclusion

We have designed and simulated the performance of a double nano-grating plasmonic MSM-PD device for the enhancement of light transmission through a subwavelength aperture. FDTD method has been used to optimize the various device parameters, namely the bottom nano-grating height, the grating duty cycle, and nano-grating periodicity for maximum light transmission enhancement. Simulation results have shown that the plasmonic MSM-PD structures with single and double gratings can attain a maximum light transmission enhancement factor of 8- and 21-times better than that of a conventional MSM-PD. Experimentally, we have demonstrated enhancement of more than 4 times of the photocurrent due to nano-structuring the top MSM-PD fingers with nano-gratings in comparison with the conventional MSM-PDs. These simulation and experimental results are useful for the development of high-responsivity-bandwidth MSM-PDs.

V. Acknowledgement

This research was supported by Edith Cowan University and the World-Class University Program funded by the Ministry of Education, Science, and Technology through the National Research Foundation of Korea (R31-10026).

VI. References

[1] J. B. D. Soole and H. Schumacher, "InGaAs metal-semiconductor-metal photodetectors for long wavelength optical communication," *IEEE J. Quantum Electron.*, vol. 27, no. 3, pp. 737–752, Mar. 1991.

[2] M. Ito and O. Wada, "Low dark current GaAs metal-semiconductormetal (MSM) photodiodes using WSi contacts," *IEEE J. Quantum Electron.*, vol. QE-22, no. 7, pp. 1073–1077, Jul. 1986.

[3] S. Y. Chou, Y. Liu, and P. B. Fischer, "Tera-hertz GaAs metal-semiconductor-metal photodetectors with 25 nm finger spacing and finger width" Appl. Phys. Lett., 61 (4), 27 Jul. 1992.

[4] S. Averine, et al., "Geometry optimization of interdigitated Schottky-barrier metal–semiconductor–metal photodiode structures," Solid-State Electronics, vol. 45, pp. 441- 446, March 2002.

[5] T. W. Ebbesen, H. J. Lezec, H.F. Ghaemi, T. Thio and P. A. Wolff, "Extraordinary optical transmission through sub-wavelength hole arrays," Nature, Vol 391, 667–669, 1998.

[6] W. Li-Chun, D. L. Ni, N. Yue-Ping and G. Shang-Qing, "Extraordinary optical transmission through metal gratings with single and double grooved surfaces," Chin. Phys. B Vol. 19, No. 1 017303, 2010.

[7] R. D. Bhat, N. C. Panoiu, S. R. Brueck, and R. M. Osgood, "Enhancing the signal-to-noise ratio of an infrared photodetector with a circular metal grating," Opt. Exp, Vol. 16, No. 7 , 4588, Mar. 2008.

[8] F. J. García-Vidal and, L. Martín-Moreno, "Transmission and focusing of light in one-dimensional periodically nanostructured metals," Phys. Rev. B, Vol. 66, Issue 155412, 2002.

[9] G. Lévêque, O. J. F. Martin, and J. Weiner, "Transient behavior of surface plasmon polaritons scattered at a subwavelength groove," Phys. Rev. B, Vol. 76, 155418, Oct. 2007.

[10] Z. F. Yu, et al., "Design of midinfrared photodetectors enhanced by surface plasmons on grating structures," Appl. Phys. Lett. vol. 89, Oct 9 2006.

[11] W. Wu, et al., "Plasmonic enhanced quantum well infrared photodetector with high detectivity," Appl. Phys. Lett. vol. 96, Apr 19 2010.

[12] S. Collin, F. Pardo, R. Teissier, and J. Pelouard, "Efficient light absorption in metal–semiconductor–metal nanostructures," *Appl. Phys. Lett.*, vol. 85(2), Jul. 2004.

[13] A. Karar, N. Das, C. L. Tan, K. Alameh, and Y. T. Lee, "Design of High-Sensitivity Plasmonics-Assisted GaAs Metal-Semiconductor-Metal Photodetectors", In proceedings 7th International Symposium on High Capacity Optical Networks & Enabling Technologies (HONET-2010), Cairo, Egypt, December 19-21, 2010.

[14] T. Ishi, J. Fujikata, K. Makita, T. Baba, and K. Ohashi, "Si Nano-Photodiode with a Surface Plasmon Antenna," Jpn. J. Appl. Phys., Part 2 44, L364, 2005.

[15] http://www.optiwave.com/products/fdtd_overview.html.

[16] Aleksandar D. Rakic, Aleksandra B. Djurišic, Jovan M. Elazar, and Marian L. Majewski, Optical properties of metallic films for vertical-cavity optoelectronic devices, Applied Optics, 37, 22, 5271-5283, 1998.

[17] E. D. Palik, "Galllium Arsenide (GaAs)" in Handbook of Optical Constants of Solids, E. D. Palik, ed. (Academic, San Diego, USA, 1985).

[18] F. J. Garcia-Vidal, et al., "Focusing light with a single subwavelength aperture flanked by surface corrugations," Appl. Phys. Lett., vol. 83, pp. 4500-4502, 2003.

[19] G. Gay, O. Alloschery, B.V. Lesegno, J. Weiner, and H. J. Lezec. "Surface Wave Generation and Propagation on Metallic Subwavelength Structures Measured by Far-Field Interferometry," Phys. Rev. Lett, 96(21):213901, Jun. 2006.

[20] Narottam Das, Ayman Karar, Mikhail Vasiliev, Chee Leong Tan, Kamal Alameh and Yong Tak Lee, "Analysis of nano-grating-assisted light absorption enhancement in metal-semiconductor-metal photodetectors patterned using focused ion-beam lithography", Optics Communications 284, 1694–1700, 2011.

[21] Narottam Das, Ayman Karar, Chee Leong Tan, Kamal Alameh and Yong Tak Lee, "Impact of Metal Nano-Grating Phase-Shift on Plasmonic MSM Photodetectors", In proceedings 7th International Symposium on High Capacity Optical Networks & Enabling Technologies (HONET-2010), Cairo, Egypt, December 19-21, 2010.